The 11th Canadian Conference on Earthquake Engineering
Canadian Association for Earthquake Engineering
11CCEE

NONLINEAR ANALYSIS OF SHEAR WALL FOUNDATION ROCKING

Poureya BAZARGANI
Structural Engineering EIT, Ausenco Ltd., Canada
pouryab@yahoo.com

Perry ADEBAR
Professor of Structural Engineering, University of British Columbia, Canada
adebar@civil.ubc.ca

Ron DeVALL
Senior Structural Engineer, Read Jones Christoffersen Ltd., Canada
RDeVall@rjc.ca

Donald ANDERSON
Emeritus Professor of Structural Engineering, University of British Columbia, Canada
dla@civil.ubc.ca

ABSTRACT: As part of a project to revise the foundation design provisions for the 2015 National Building Code of Canada (NBCC), a series of Nonlinear Time-History Analysis (NTHA) was performed on shear walls supported on foundations that are free to rotate ("rock"). The nonlinear compressive response of soil and separation of the footing from the underlying soil was modeled using the QzSimple1 material in OpenSees. Ten ground motion records were modified to fit the 2475-year return period UHS for Vancouver and used to analyze various wall-foundation systems, while the variation in foundation response was investigated using uniformly scaled records. The two sets of records gave similar mean results. A series of pilot studies was conducted on 10-storey walls to investigate certain wall and foundation parameters such as soil strength and stiffness, and the amount of radiation damping associated with the soil. Accounting for foundation rotation generally increases building drifts. The increase in building drifts due to foundation rotation is not very sensitive to the soil properties used; however, the permanent displacements of the soil depend on soil strength and stiffness.

1. Introduction

It is a common for structural engineers to model shear walls on spread footings as having fully fixed boundary conditions such that no rotation can occur in the foundation. In reality however, no matter how large a foundation is, some rotation will occur when the shear wall is subjected to large lateral loads. Significant foundation rotation may take place under seismic loading because of either uplift of the footing or compressive displacement of the underlying soil, or in most circumstances, a combination of the two. Rotation of the shear wall foundation changes the displacement profile of the building and results in additional deformation demands on the gravity-load resisting system of the building. Therefore, quantifying the amount of foundation rotation is essential to ensuring that the gravity-load system is capable of resisting the deformation demands from and earthquake.

Previous work by Housner (1963) and Priestley et al. (1978) showed that accounting for the flexibility in the foundation can be used as an effective way of resisting earthquake effects. Gazetas (1991) presented algebraic formulas for stiffness and damping coefficients of surface and embedded foundations on/in an elastic half-space. Sophisticated nonlinear modeling techniques such as the use of macro-elements, 3D Finite Element (FE) analysis of the soil, and Beam on Nonlinear Winkler Foundation (BNWF) have been

developed and used. Simple design-oriented methods for accounting for foundation rotation have been formulated such as the ones outlined in the ASCE41 guidelines. However, the existing vast literature on foundation rotation has been mostly focused on soil-foundation interaction with little or no emphasis on the nonlinear interaction between the superstructure and the foundation. Anderson (2003) carried out a series of analysis of 7, 15, and 30-story elastic walls on footings supported on a series of Elastic Perfectly-Plastic (EPP) springs. He showed that shorter walls and foundations with larger vertical loads are more susceptible to rocking rotations. Filiatrault et al. (1991) published results of an analytical study of an EPP 21-storey core wall on a foundation made up of a series of EPP springs, subjected to dynamic shaking. Le Bec (2009) modeled a 10-storey shear wall made up of nonlinear fibre elements supported on two types of sand with three foundation sizes for each soil.

The literature on the influence of foundation rotation on the response of the superstructure and particularly shear walls is scarce. The work of Anderson (2003) focused solely on elastic shear walls. Even though the study by Filiatrault et al. (1991) considered the interaction between the nonlinear behaviours of the wall and the foundation, only one wall-foundation strength combination was studied and the nonlinear models chosen were simple EPP models. Despite Le Bec (2009) using sophisticated numerical tools to model walls with rocking foundations, his study included a very limited number of wall-foundation-soil type combinations. The need for a study in which the interaction of the nonlinear behaviours of the wall and the foundation is considered through a range of relative wall-to-foundation strengths and on various soil types is obvious.

2. Analysis and Modelling Method

Numerous analytical tools for studying soil-structure interaction have been developed. Among them, the use of nonlinear Winkler springs seems to have gained more popularity as it is relatively simple to understand and implement. This modeling technique has been used by many researchers in the past including Harden et al. (2005), Ugalde et al. (2010), Anderson (2003), Filiatrault et al. (1991), and Le Bec (2003). Nonlinear Winkler springs along with gap elements for the separation between the soil and the footing were used in the current study to model the nonlinear rotational behaviour of the foundation.

10-story walls with cross-sectional dimensions shown in Fig. 1 were constructed using nonlinear concrete and reinforcing steel fibres in OpenSees. Concrete04 material was used for concrete fibres with f'_c set to 30 MPa. Steel01 material (bilinear stress-strain relationship) was used to model the reinforcing steel fibres. Yield strength of 400 MPa, elastic modulus of 200 GPa and 1% strain hardening were assumed. Seismic mass was lumped at floor slab levels and adjusted such that the elastic first mode period of vibration of the fixed-base 10-story wall was 1.0 sec, as this is a typical value for 10-story buildings. The axial load in the wall was assumed to vary linearly over the height of the wall. The Mass Ratio (MR), equal to the ratio of the gravity load applied to the foundation to the total weight of the structure (generating lateral seismic loads applied to the wall), was 40%, i.e., MR = 0.4.

Elastic bending moment demand of the fixed-base wall was calculated from Response Spectrum Analysis (RSA) using the UHS (see Fig. 3) and called M_{RSA}. The amount of vertical steel in the wall was varied as needed to create walls with various bending strengths. Wall bending strength was then expressed as a strength ratio R_w defined as follows.

$$R_w = \frac{M_{RSA}}{M_y} \tag{1}$$

Where M_y is the wall strength. A larger R_w indicates a weaker wall and vice versa.

The footing was fixed against horizontal movement as shown schematically in Fig. 1 ignoring sliding and the friction effect between the thickness of the footing and the soil. In reality, the portion of the footing directly underneath the shear wall will be stiffened against out-of-plane flexure by the wall itself. Foundation overhangs are usually short relative to the depth of the footing. They are designed to remain elastic and therefore, do not deform significantly during foundation rocking. Anderson (2003) did some initial analysis with the walls sitting on elastic footings and discovered that the results were very similar to the cases were the footings were assumed to be perfectly rigid. In this study, wall footings were modeled as rigid elements to eliminate any flexural deformation of the footing.

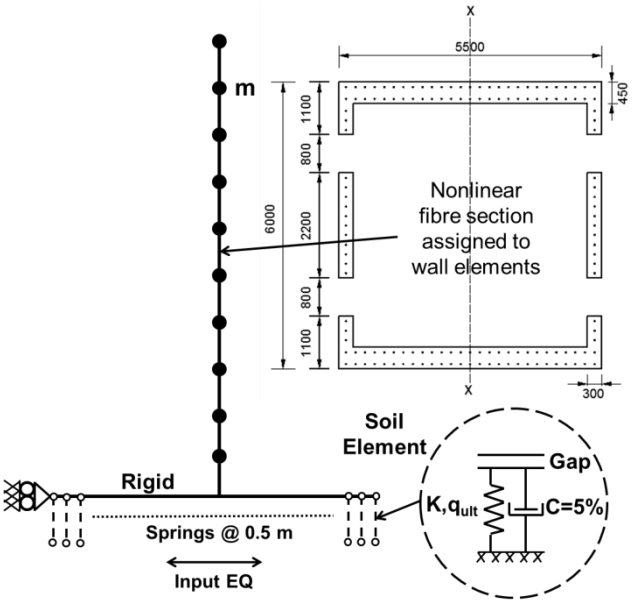

Fig. 1 – Schematic view of 2D modeling of shear walls with a flexible foundation.

Nonlinear Winkler springs were used to simulate the compressive behaviour of the soil. QzSimple1 material model in OpenSees was chosen for the Winkler springs. Each soil element constructed using this material was composed of a nonlinear spring in parallel with a viscous damper both in series with a gap element that connects to the footing (see insert in Fig. 1). Fig. 2 shows the non-dimensional backbone curves of the QzSimple1 material formulated for clays and sands. Unloading occurs along a line parallel to the initial slope of the curves. The inputs to the QzSimple1 model are the ultimate bearing capacity (q_{ult}) and the compressive displacement needed to mobilize 50% of the ultimate bearing capacity (Z_{50}). Soil suction was neglected.

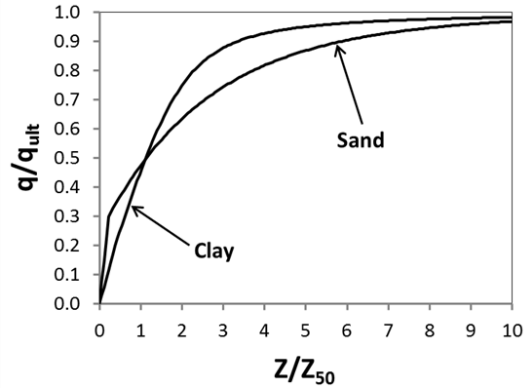

Fig. 2 – Dimensionless backbone curves for QzSimple1 material in OpenSees used as Winkler springs to simulate soil-structure interaction.

Gazetas (1991) first introduced equations for computing the uncoupled elastic rotational stiffness of a rigid foundation sitting on an elastic half-space medium. Gazetas' formulations for the uncoupled rotational stiffness $K'_{\theta y}$of a rectangular foundation is as follows.

$$K'_{\theta y} = \frac{G}{1-\nu} I_y^{0.75} \left[3\left(\frac{L}{B}\right)^{0.15}\right] \quad (2)$$

In the equations above, G is the elastic shear modulus of the soil, v is the Poisson's ratio, L is the foundation length, B is the foundation width, and I_y is equal to $BL^3/12$. This stiffness is the surface stiffness as if the foundation is placed on the surface of the soil. To consider the effect of embedment on foundation stiffness, Gazetas proposed a multiplier to be applied to the surface stiffness.

$$e_{\theta y} = 1 + 0.92\left(\frac{2d}{L}\right)^{0.62}\left[1.5 + \left(\frac{2d}{L}\right)^{1.9}\left(\frac{d}{D}\right)^{-0.60}\right] \quad (3)$$

Where d is the thickness of the foundation and D is the depth at which the foundation is placed. The total uncoupled stiffness would then be.

$$K_{\theta y} = e_{\theta y} K'_{\theta y} \quad (4)$$

To use the QzSimple1 material for a given soil, the soils ultimate bearing capacity was used as q_{ult}. Z_{50} was then adjusted such that the uniformly spread soil springs resulted in an initial elastic rotational stiffness for the foundation given by Eq. 4 for the chosen value of soil shear modulus (G).

The overturning capacity of the foundation can be expressed as follows:

$$R_f = \frac{M_{RSA}}{M_{oc}} \quad (5)$$

where M_{RSA} is the elastic bending moment demand from Response Spectrum Analysis (RSA) and M_{oc} is the factored foundation overturning capacity calculated assuming a rectangular stress block of intensity equal to $0.5q_{ult}$ at the "toe" of the foundation required to balance the vertical load on the foundation.

3. Spectrally-matched vs. Uniformly-scaled Ground Motions

Although spectrally-matched records are good for estimating the mean response of a structure, certain natural characteristics of the motion are lost during the matching process. Gazetas and Apostolou (2004) concluded that "the nature of seismic excitation (specifically its frequency composition and, especially, the presence of a sequence of long duration impulsive cycles) is the controlling factor of the response of a specific system." To study the scatter in the response of shear wall foundations, 10 ground motions were uniformly scaled to fit the UHS in the period range of 0.5 to 2.5 sec (see Fig. 3a). The same original records were also spectrally matched to the UHS (see Fig. 3b). The spectra for the uniformly-scaled records deviate from the UHS; however, the average of the 10 spectra is consistent with the UHS.

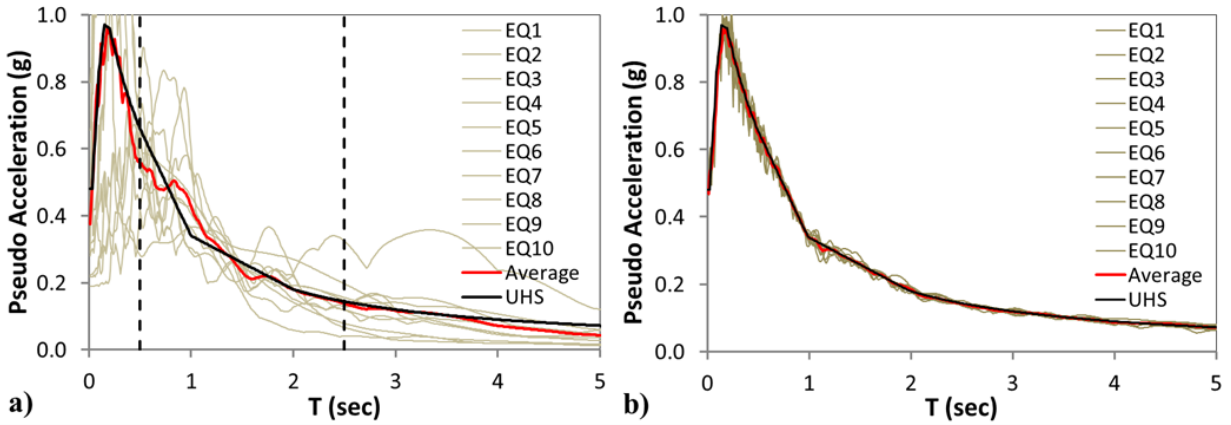

Fig. 3 – Acceleration spectra of ten ground motion records used in the NTHA: a) uniformly-scaled, and b) spectrally-matched.

A 10-storey wall with R_w = 1.3 was modeled on five different foundations supported on a dense sand with q_{ult} = 1.6 MPa and G = 578 MPa. A strong (and stiff) soil was chosen as it results in smaller foundations, and a strong wall was chosen as it results in larger movements in the soil. The five wall-foundation systems were subjected to both the spectrally-matched and uniformly-scaled records.

Figure 4 summarizes the mean (average) and maximum top-wall displacements (and global drift) from the NTHA along with the standard deviations. As expected, the maximum response and standard deviation from the uniformly-scaled ground motions is larger than obtained using the spectrally-matched records. Unlike spectrally-matched records, analysis using uniformly-scaled records provide a measure of the scatter in the top-wall displacement. The mean response from both the spectrally-matched and the uniformly-scaled ground motions are very similar. Thus spectrally-matched ground motions are used for the remainder of this study to examine the mean response.

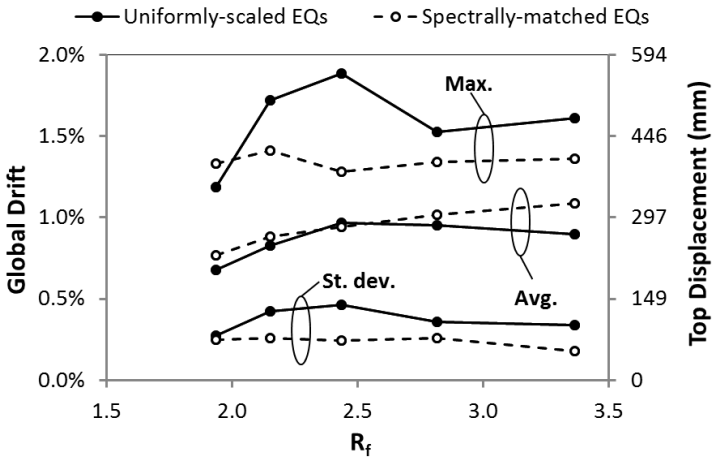

Fig. 4 – Comparison between top-wall displacement (global drift) of a 10-story wall with R_w = 2.0 obtained from NTHA using spectrally-matched and uniformly-scaled ground motions.

4. Effect of Soil Damping

The viscous damper embedded in the QzSimple1 material in OpenSees and shown in Fig. 1 is intended to capture radiation damping due to dissipation of energy through the soil upon foundation impact. Too little damping can result in unrealistic large foundation rotations while too much damping can underestimate foundation rotation and hence wall maximum displacement. The amount of damping assigned to the soil elements is therefore an important parameter.

Evidence of radiation damping has been observed by other researchers in experiments. In the TRISEE test on high density (HD) and low density (LD) Ticino sand, Negro et al. (1998) measured damping ratios between 1% and 6% using the initial elastic rotational stiffness. In centrifuge tests carried out on foundations supported on sand and clay, Gajan and Kutter (2008) observed damping ratios between 15% and 30% using the foundation's secant stiffness. In a series of tests on Auckland residual clay, Algie (2011) observed damping ratios as high as 50% with an average of 25% again using the secant stiffness of the foundation. As foundations start to rotate, a smaller length of the foundation is in contact with the soil and the foundation rotational stiffness decreases. Therefore, damping ratios calculated using secant stiffness of the foundation are much larger than those calculated from the initial elastic stiffness. Negro et al. (1998) report damping ratios between 14% and 32% for the same TRISEE tests using the foundation's secant stiffness instead of the 1% to 6% range. This explains the seemingly large damping ratios observed by Gajan and Kutter (2008) and Algie (2011). The viscous damping incorporated in the QzSimple1 material is expressed in terms of the initial elastic stiffness. A damping ratio 0f 5% was used in this study to account for foundation radiation damping.

To further investigate the appropriate level of damping for the NTHA, a pilot study was performed on a 10-story wall with R_w = 2.0 supported on a 12.5 m square foundation was modeled on a soil with q_{ult} = 1.54 MPa and G = 126 MPa. The level of damping assigned to the soil elements was increased from 0% to 30% in increments of 5%. For each level of damping in the soil, NTHA was done with the 10 spectrally-matched ground motions. Fig. 5 shows the average of top wall displacements from the 10 ground motions. Top wall displacement decreased steadily as soil damping was increased. When no damping was associated with the QzSimple1 soil elements, for some ground motions, top wall displacement kept increasing even after the strong shaking was over. This unrealistically undamped behaviour was eliminated when as little as 5% damping was assigned to the soil elements. Higher values of damping resulted in less rocking of the foundation.

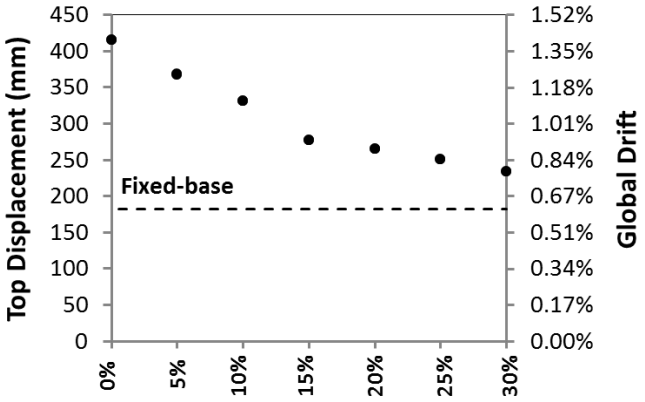

Fig. 5 – Influence of soil damping level on average top displacement (and global drift) of a 10-story wall with R_w = 2.0 supported on a 12.5 m square foundation on medium-density sand.

5. Sensitivity of Soil Properties

A pilot study was done to investigate the sensitivity of shear wall and foundation response to the assumed soil properties. The chosen properties (Table 1) represent a broad set of soils ranging from upper-bound clays to a variety of sands and lower-bound tills. A 10-story wall with R_w = 2.0 supported on a 12.5 m square foundation was modeled on each soil type. Foundation sizes were chosen to result in values of R_f between 2.0 and 4.0 for the values of q_{ult} shown in Table 1 to ensure large nonlinear rotations of the foundation. The vertical (gravity) load supported by the foundation was 41550 kN.

Table 1 - Soil properties used in parametric study on soil properties.

	Soil 1	Soil 2	Soil 3	Soil 4	Soil 5
E (MPa)	107	187	327	571	1000
G (MPa)	43	73	126	215	370
v	0.25	0.28	0.30	0.33	0.35
q_{ult} (kPa)	501	877	1535	2686	4700

5.1. Soil Type

The foundation overturning moment – rotation response of the 12.5 m square foundations on the five soils presented in Table 1 are given in Fig. 6a. The initial stiffness of the springs was adjusted such that the initial elastic rotational stiffness of the foundation matched the stiffness given by Gazetas. The figure demonstrates how diverse the soils are in terms of stiffness and strength. Overturning capacities of the foundations (vary by factor of 2.5 are less diverse than the bearing capacities of the five soils (vary by factor of 9.4. This is because the overturning capacity is equal to the applied vertical load (constant) times a lever-arm that depends on both the overall footing length (constant) and the length of uniform bearing stress needed to support the vertical load.

Figure 6b presents the average top-wall displacement and global drift from the 10 ground motions. As the soils get softer and weaker, wall displacements generally increase. One exception to this is Soil 1, which is softer and weaker than Soil 2 and Soil 3; but experienced smaller maximum top-wall displacements. The explanation for this behaviour can be found in the soil maximum displacement profiles given in Fig. 7. Going from Soil 5 (smallest displacements) to Soil 2 (solid line), the displacements at the “toe” of the foundation increase as the soil becomes weaker, i.e., the “toe” of the foundation digs in more. Also, the slopes of the soil deformation envelopes near the “toe” of the foundations, which are equal to the maximum footing rotation, increase. When the lateral load is removed from the wall, the footing is supported only on the central part of the footing immediately below the wall because of the permanent soil deformation at the “toe.” Soil 1 is so weak that the applied vertical load cannot be supported by a short length of the footing immediately under the wall and thus the footing moves down until there is sufficient length of footing supporting the vertical load. The result is less rounding of the soil surface, a

smaller slope in the soil displacement profile at the “toe” of the foundation, less foundation rotation, and less top-wall displacement.

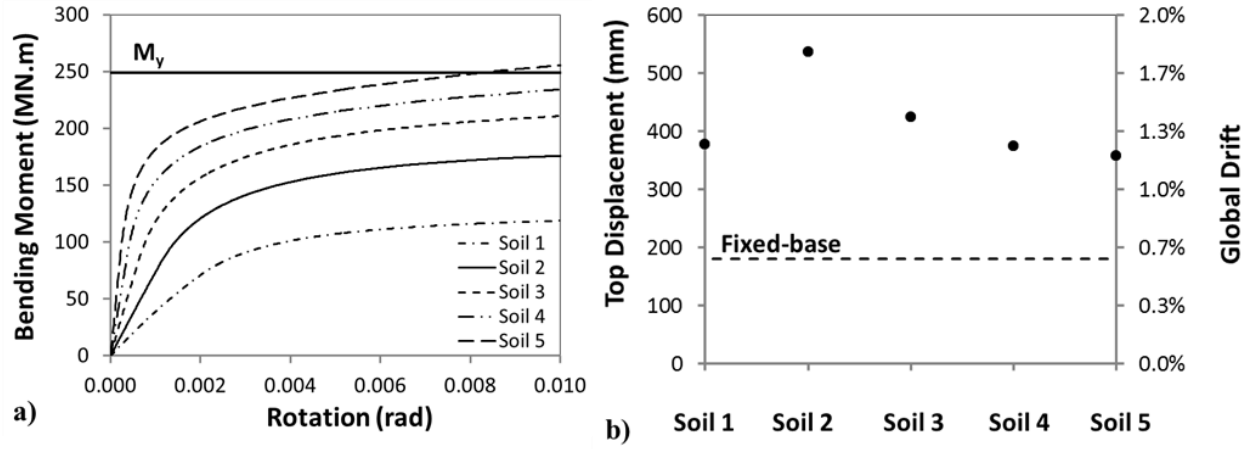

Fig. 6 – a) Foundation bending moment-rotation response of a 12.5 m square foundation on 5 different soil types, b) average of top-wall displacement (global drift) of a 10-story wall with R_w = 2.0 supported on a 12.5 m square foundation on 5 types of soil.

Another contributor to Soil 1 resulting in less top-wall displacement than Soil 2 is the portion of top displacement resulting from flexural deformation of the wall. Due to the reduced bearing capacity of Soil 1, the overturning capacity of the foundation is reduced and thus the maximum bending moment that can be induced in the shear wall is also reduced. The smaller flexural deformations of the wall also contribute to smaller top-wall displacements.

For all five types of soils, the top displacements of the wall increased considerably compared to the fixed-base case (see Fig. 6b). The increase was more than 200% for the wall on Soil 2. The difference in wall top displacements among the different types of soil however is small bearing in mind the extreme diversity in soil strength and stiffness among the five soils. This suggests that behaviour of shear walls with rocking foundations is not very sensitive to the properties of the soil underlying the foundation.

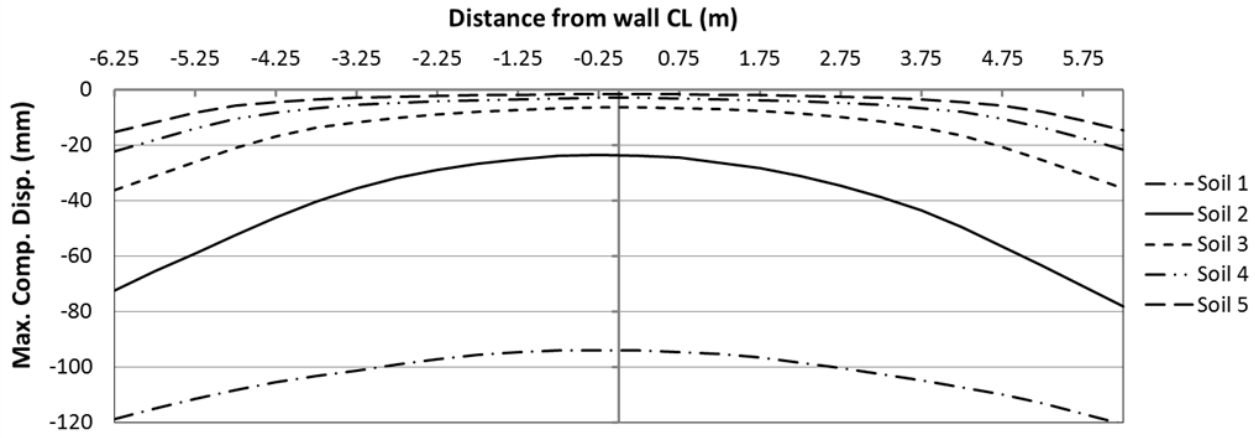

Fig. 7 – Average soil displacement profiles for a 12.5 m foundation on various soil types supporting a 10-story wall with R_w = 2.0.

5.2. Soil Stiffness

To investigate the effect of soil stiffness only on the behaviour of shear walls with rotating foundations independent of the soil ultimate bearing capacity, the five soils shown in Table 1 were modified such that they all had the same ultimate bearing capacity as Soil 3 (1535 kPa). The resulting foundation bending moment-rotation responses are plotted in Fig. 8a. Because the ultimate bearing capacity of all five soils

was the same, all curves will eventually result in the same overturning capacity even though the softer soils will need a larger rotation to develop the full overturning capacity. Average of wall top displacement and global drift envelopes are given in Fig. 8b. As expected, the top-wall displacement increases as the soil gets softer, and the softest soil results in the largest top-wall displacement.

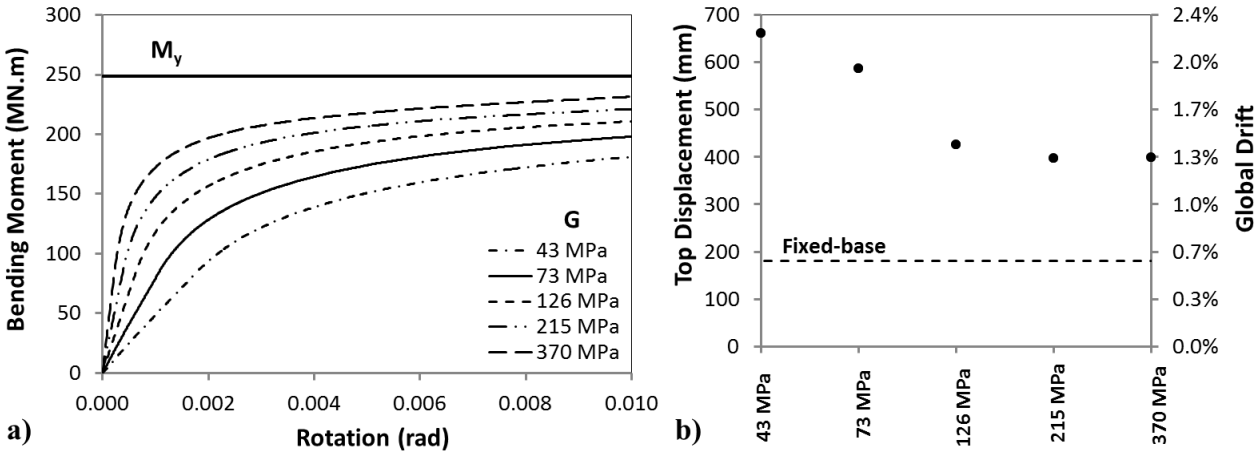

Fig. 8 – a) Foundation bending moment-rotation response of a 12.5 m square foundation on 5 soils with q_{ult} = 1.54 MPa and various stiffnesses, b) average of top-wall displacement and global drift envelopes of a 10-story wall with R_w = 2.0 supported on the foundations.

While the soil stiffness does influence the displacement of shear walls that are support by the foundations, the influence of the soil stiffness is less than may be expected. The stiffness of the soil was reduced by almost a factor of 8.6, while the increase in top-wall displacement from the fixed-base case only increased by a factor of 2.2. It is therefore concluded that lateral displacement of shear walls with rotating foundations is not critically sensitive to the assumed soil stiffness.

5.3. Soil Ultimate Bearing Capacity

Soil ultimate bearing capacity was also investigated independent of soil stiffness, and five different soils were again considered. All soils had the stiffness of Soil 3 shown in Table 1 but the ultimate bearing capacities ranged from that of Soil 1 to Soil 5. Overturning moment – rotation response of the foundation on the five soils with various ultimate bearing capacities is shown in Fig. 9a. Note how the initial slope of the curves is identical for all five curves with the only difference being their overturning capacities.

Despite the great difference among the five soils in terms of ultimate bearing capacity, the difference in the foundation bending moment-rotation responses is much less drastic. The foundations on the first three strongest soils have a very similar response while there is a gap between the responses of foundations on the two weaker soils. Foundation moment – rotation responses certainly did not vary in proportion to the soil ultimate bearing capacity. This is again because the overturning capacity is equal to the applied vertical load (constant) times a lever-arm that depends on both the overall footing length (constant) and the length of uniform bearing stress needed to support the vertical load.

Fig. 9b shows the results of the NTHA of the wall on the five soils with different ultimate bearing capacities. It is striking how the four strongest soils result in similar top wall displacements while the wall on the weakest soil has the lowest top displacement. This observation can again be explained by looking at the maximum soil displacement profiles shown in Fig. 10. The maximum soil displacement profiles of the four stronger soils is quite rounded because the soils were strong enough to support the vertical load from the wall over a smaller bearing area. This resulted in the maximum soil compressive displacement profile to be steeper near the “toes” of the foundation and increase maximum foundation rotation and consequently, wall top displacement. The weakest soil on the other hand was so weak that it required a very large area of soil bearing to withstand the vertical load which resulted in large compressive displacements over much larger areas under the foundation. This made the maximum soil compressive displacement profile to be quite flat and reduced maximum foundation rotation. As a result, top-wall displacement on the weakest soil was smaller than those on all stronger soils.

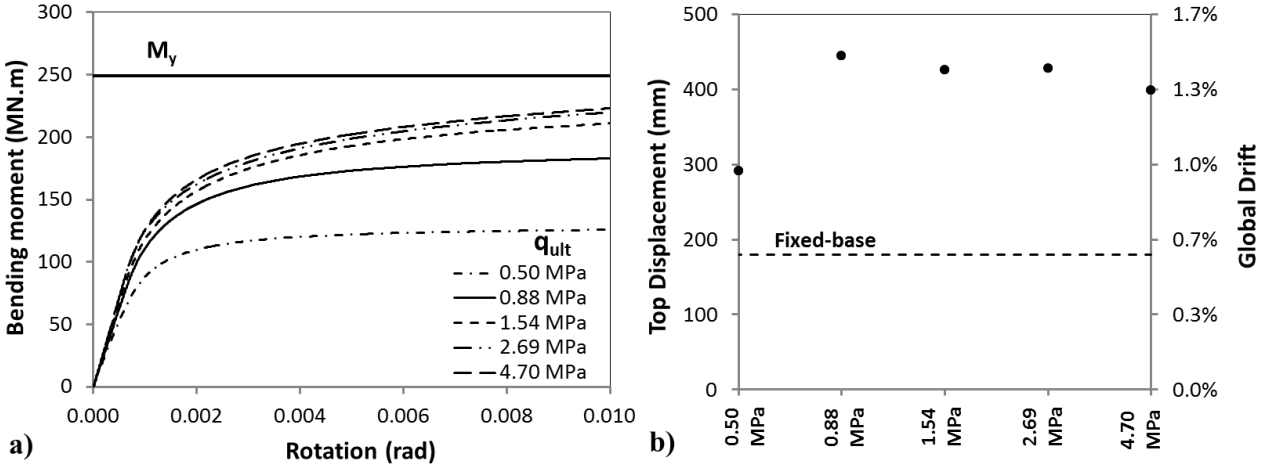

Fig. 9 – a) Foundation bending moment – rotation response of a 12.5 m square foundation on 5 soils with *G* = 126 MPa and various bearing capacities, b) average top-wall displacement of a 10-story wall with R_w = 2.0 supported on the foundations.

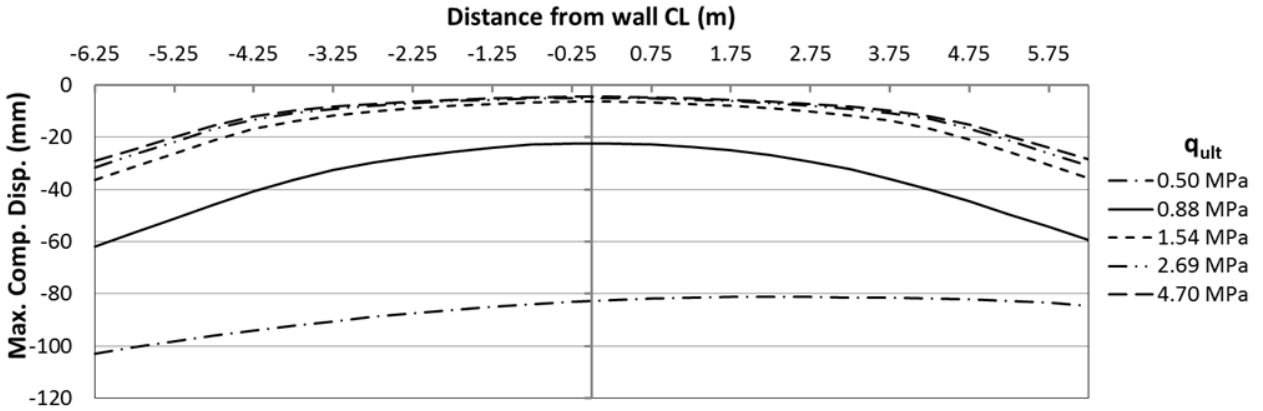

Fig. 10 – Average of maximum soil displacement profiles for a 12.5 m foundation on 5 soils with various ultimate bearing capacities supporting a 10-story wall with R_w = 2.0.

It is therefore concluded that decreasing the soil ultimate bearing capacity initially increases top wall displacement but as the soil gets very weak, top wall displacement start to decrease as the maximum compressive displacement profile of the soil becomes flatter reducing foundation rotation. Despite the extreme variation in soil strength (almost by a factor of 10), the relative increase in top-wall displacement compared to the fixed-base case was only 2.4. Hence, top-wall displacement of shear walls are not overly sensitive to soil bearing strength.

6. Conclusions

The main conclusions from this pilot study are as follows:

- The mean wall response calculated using spectrally-matched ground motions agreed well with that obtained using uniformly-scaled ground motions; however, as expected, the scatter of the results are much less.
- Maximum top-wall displacement and foundation rotation proved to be sensitive to soil damping. 5% damping (calculated using the initial elastic rotational stiffness of the foundation) was found to be the minimum amount of damping required to eliminate unrealistic undamped oscillation of the foundation.
- The response of shear walls accounting for foundation rotation was found to be surprisingly insensitive to the assumed properties of the soil. A parametric study on the effect of soil properties revealed that, for a given footing size, the maximum soil compressive displacement profile was steeper near the “toe” areas for stronger and stiffer soils resulting in large maximum foundation rotation. As the soil got weaker

and softer, a larger soil bearing area was needed to support the vertical load on the footing resulting in larger soil compression but a more flat maximum soil compressive displacement profile. Footings on extremely weak or soft soils experience smaller foundation rotations for this reason.

The pilot studies presented in this publication have been used to design a comprehensive series of NTHA of shear walls with rocking foundations considering a broad range of wall-footing-soil combinations. In the study, five shear walls (one elastic and four nonlinear with various strengths) are each modeled on five or seven different foundation sizes supported on five types of soil (one clay, three types of sand with various densities, and rock). More than 125 structures (wall strength-footing size-soil type combinations) are analyzed through more than 1500 individual NTHA runs. Results of that work are soon to be published.

7. References

Algie, T. B. (2011). "Nonlinear Rotational Behaviour of Shallow Foundations on Cohesive Soil", *Doctoral Thesis*, The University of Auckland, Department of Civil and Environmental Engineering, New Zealand.

Anderson, D. L. (2003). "Effect of Foundation Rocking on the Seismic Response of Shear Walls", *Canadian Journal of Civil Engineering*, 30(2): 360-365.

Filiatrault, A., Anderson, D.L., and DeVall, R.H. (1991). "Effect of a weak foundation on the seismic response of core wall type buildings", *Canadian Journal of Civil Engineering*, 19: 530-539.

Gajan, S., and Kutter, B. L. (2008). "Capacity, settlement, and energy dissipation of shallow footings subjected to rocking." *J. Geotech. Geoenviron. Eng*., 134(8): 1129–1141.

Gazetas, G. (1991). "FORMULAS AND CHARTS FOR IMPEDANCES OF SURFACE AND EMBEDDED FOUNDATIONS", *Journal of Geotechnical Engineering*, 117(9): 1363-81.

Gazetas, G., and Apostolou, M. (2004). "Nonlinear Soil–Structure Interaction:Foundation Uplifting and Soil Yielding", *Proceedings Third UJNR Workshop on Soil-Structure Interaction*, March 29-30, 2004, Menlo Park, California, USA.

Harden, C., Hutchinson, T., Martin, G. R., and Kutter, B. L. (2005). "Numerical modeling of the nonlinear cyclic response of shallow foundations", *PEER Report 2005/04*, U.C., Berkeley.

Housner, G. W. (1963). "The behaviour of inverted pendulum structures during earthquakes", *Bulletin of the Seismological Society of America*, 53(2): 403-417.

Le Bec, A. (2009). "Effects of rocking of shallow foundation on seismic response of reinforced concrete shear walls", *M.Sc. Thesis*, CGM Dept., Ecole Polytechnique de Montréal, Montréal, QC (In French).

Negro, P., Verzeletti, G., Molina, J., Pedretti, S., Lo Presti, D., and Pedroni, S. (1998). "Large-scale geotechnical experiments on soil–foundation interaction", *Special publication No. I.98.73*, Ispra, Italy: Joint Research Center, European Commission.

Priestley, M. J. N., Evison, R. J., and Carr, A. J. (1978). "Seismic response of structures free to rock on their foundations", *Bulleting of the New Zeland national society for earthquake engineering*, 11(3): 141-150.

Ugalde, J. A., Kutter, B. L., and Jeremic, B. (2010). "Rocking Response of Bridges on Shallow Foundations", *PEER Report 2010/101*, U.C., Davis.